# Expanding the Field Range of PHE Sensors for Increased Industrial Applicability

Department of Physics
Faculty of Exact Sciences
Bar-Ilan University

Bar-Ilan Institute of Nanotechnology & Advanced Materials

Daniel Lahav[1], Moty Schultz[1], Shai Amrusi[2], Asaf Grosz[2] and Lior Klein[1]

[1]Department of Physics, Institute of Nanotechnology and Advanced Materials, Bar-Ilan University, Ramat-Gan 52900, Israel
[2]Department of Electrical and Computer Engineering, Ben-Gurion University of the Negev, P.O. Box 653, Beer-Sheva 84105, Israel

## 1 Introduction

Magnetic field sensors are essential in applications such as automotive systems, industrial automation, and biomedical devices. Among these, planar Hall effect (PHE) sensors are notable for their high sensitivity (EMN in the pT/√Hz range), simple design, and compatibility with integrated circuits. However, their field range is typically limited to hundreds of μT, restricting their use in applications requiring broader field ranges.

To overcome this limitation, we manipulated the shape-induced anisotropy in elliptical PHE (EPHE) sensors by tailoring their geometry while maintaining consistent film thickness. This approach achieved a tenfold increase in the anisotropy field, extending the field range from sub-mT to tens of mT. These EPHE sensors exhibit stable performance with minimal hysteresis, making them promising for precise magnetic sensing in demanding industrial and scientific applications.

## 2 Fundamentals and Theory

### Magnetoresistance

Ferromagnetic materials exhibit a phenomenon called anisotropic magnetoresistance (AMR), in which their resistance changes depending on the orientation of their magnetization (**M**) relative to the direction of an applied electric current density (***J***).

This phenomenon gives rise to a transverse voltage as a function of the angle θ between **M** and **J**. This effect is called PHE as the magnetization, the electric current, and the transverse electric field are in the same plane.

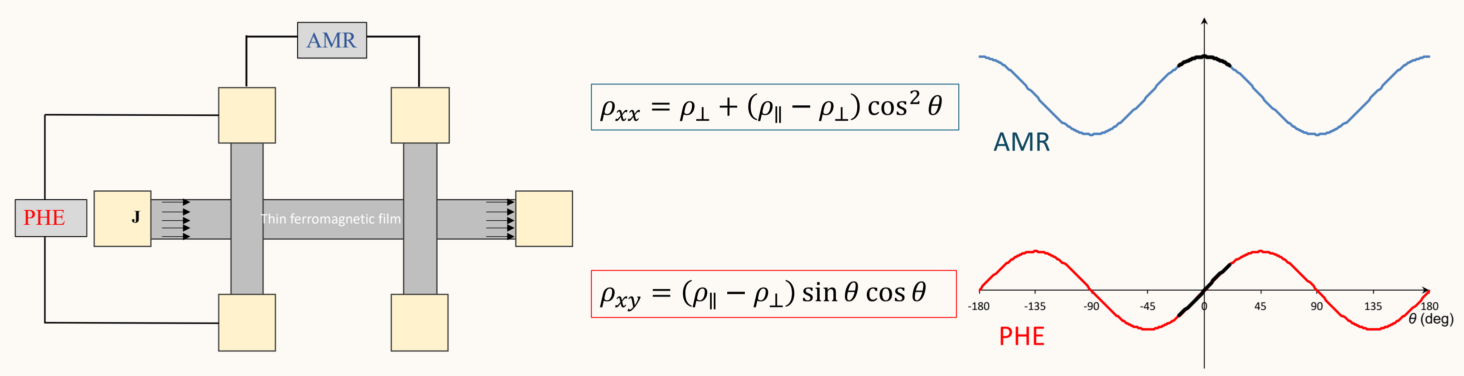


### Planar Hall Effect Sensors

PHE sensors detect magnetic fields by measuring the transverse voltage, which depends on the angle between magnetization and current. Uniform magnetization with reversible behavior, ensured by aligning magnetic anisotropy parallel to the current, is essential for optimal performance.

#### Elliptical Planar Hall Effect Sensors

The elliptical shape of PHE sensors induces uniaxial 'shape anisotropy' along the long axis, referred to as the easy axis (EA). For a flat ellipsoid with thickness *t*, major axis *a*, and minor axis *b*, the anisotropy field is:

$$H_s \sim 4\pi M_s \frac{t}{b} \sim 10807\frac{t}{b}$$

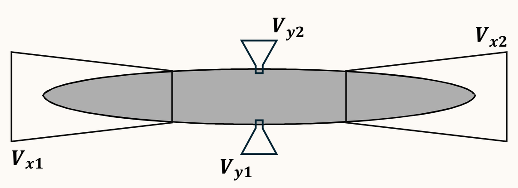


#### Sensitivity

The sensitivity ($S_y$) of a PHE sensor is the ratio of its PHE voltage ($V_y$) to the applied magnetic field in the *y*-direction ($H_y$), for a given current ($I_x$) along the EA.

When $H_y$ is small compared to the effective anisotropy field ($H_{eff}$) , the sensitivity is given by:

$$S_y = \frac{V_y}{H_y} = I_x \frac{\Delta\rho}{t}\frac{1}{H_s + H_g} = I_x \frac{\Delta\rho}{t}\frac{1}{H_{eff}}$$

Excitation current
Sensor thickness
Growth anisotropy
Shape anisotropy
Resistivity anisotropy
$\Delta\rho = (\rho_\parallel - \rho_\perp)$

#### Equivalent Magnetic Noise (EMN)

The equivalent magnetic noise (EMN, sometimes referred to as resolution) of the sensor is defined as:

$$\mathrm{EMN}(f) = \frac{e_\Sigma(f)}{S_y}$$

The total noise spectral density ($e_\Sigma$) has three main components: *1/f* noise, thermal noise (both originating from the sensor), and preamplifier noise. Namely:

$$e_\Sigma(f) = \sqrt{e_{1/f}^2 + e_T^2 + e_{amp}^2}$$

*1/f* noise dominates at low frequencies, while thermal (white) noise prevails at high frequencies.

## 3 Experimental Methodology

### A Novel EPHE Sensor with Extended Field Range

Using the dependence of shape anisotropy on *t* and *b*, theoretical calculations show that sensors with a hard axis length of 20 microns reach shape anisotropy fields exceeding 100 Oe, qualifying them as extended field range sensors.

Consequently, EPHE sensor with thickness of 200 nm and diverse hard axis lengths, specifically 200, 100, 50, and 20 microns.

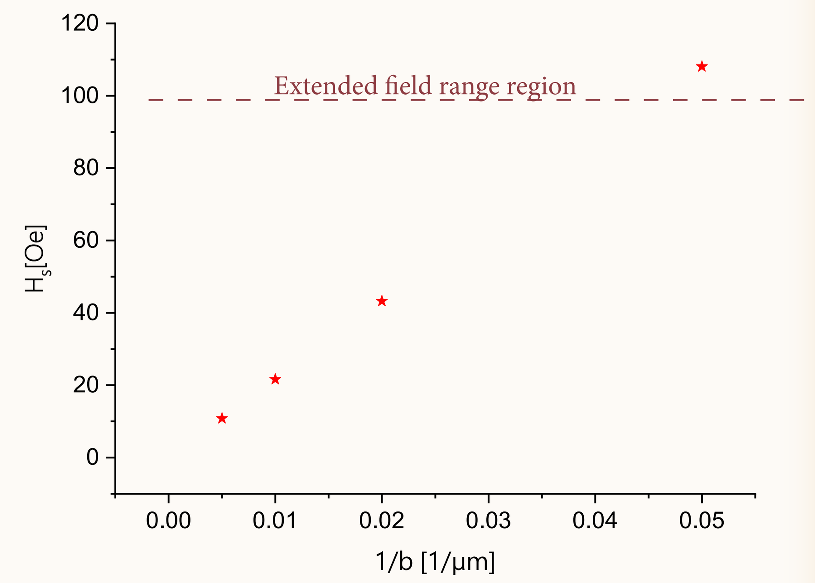


### Materials and Design

Permalloy (Py, $Ni_{80}Fe_{20}$) is used as the ferromagnetic layer for its high PHE sensitivity and low coercive field. Tantalum (Ta) acts as a seeding layer to improve crystallographic ordering and reduce coercivity, while also serving as a capping layer to protect the Py from oxidation.

A schematic of the sensor showing the major (*a*) and minor (*b*) axes of the ellipse and the gold contact pads (yellow).

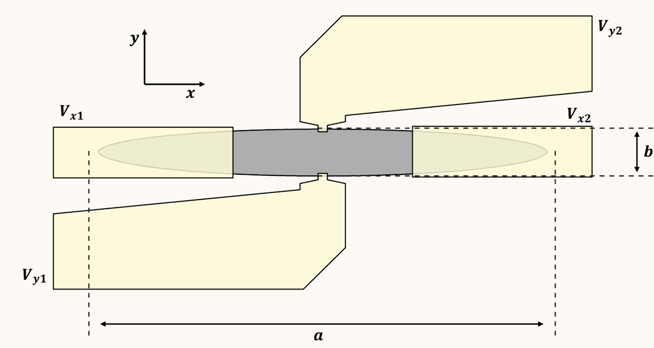


The sensor is excited with an ac current between $V_{x1}$ and $V_{x2}$, and the signal is measured at $V_{y1}$ and $V_{y2}$.

### Fabrication Process

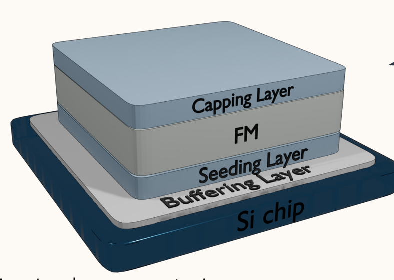


i. Ion beam sputtering.

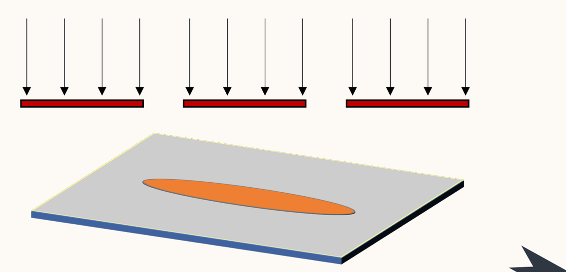

ii. First photolithography.

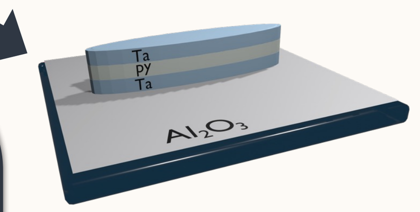


iii. Sensor layer stack after first lift-off process.

i. A stack comprising $Al_2O_3$(35nm)/Ta(15nm)/Py(200nm)/Ta(15nm) is is deposited onto a wafer using an Ion Beam Sputtering (IBS) system.

ii. Elliptical shapes are created on the wafer using photolithography.

iii. The first lift-off process is performed to reveal the elliptical shapes.

iv. Gold electrical contacts are deposited using the IBS system and patterned through photolithography.

v. The second lift-off process is conducted to expose the gold contacts.

vi. The wafer is cleaned and diced to produce the final EPHE sensors.

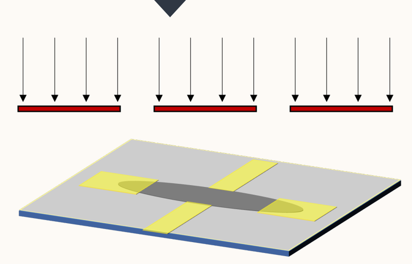

iv. Au deposition using BesTec and Photolithography using MLA150.

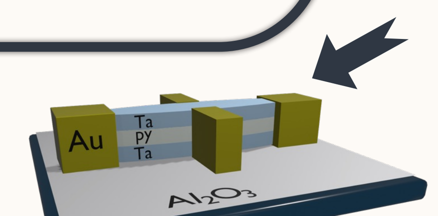


v. Sensor layer stack after second lift-off process.

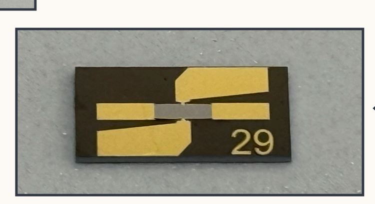


vi. EPHE sensor after cleaning and cutting the wafer.

## 4 Results and Discussion

Table 1 demonstrates that reducing the hard axis dimension (*b*) while maintaining the *a/b* ratio extends the field range of the EPHE sensor. At a constant current density, the 20-micron sensor's sensitivity is approximately 100 times lower than the 200-micron sensor, in close agreement with theoretical predictions.

| $b$ (μm) | $I$ (mA) | $H_{eff}$ (Oe) | $S_y$ (mV/T) | $\Delta R_{PHE}$ (mΩ) | $R_x$ (Ω) | $R_y$ (Ω) |
|---|---|---|---|---|---|---|
| 20 | 3 | 124.8 | 7.2 | 29 | 8.9 | 35.6 |
| 50 | 7.5 | 43.5 | 46 | 26 | 7 | 20.7 |
| 100 | 15 | 23.8 | 151.5 | 25 | 5.6 | 14.4 |
| 200 | 30 | 13.5 | 642.1 | 26 | 5.1 | 9.8 |

Table 1. Typical values of $H_{eff}$, $S_y$, $\Delta R_{PHE}$, $R_x$, and $R_y$ for EPHE sensors with varying hard axis lengths, while maintaining uniform current density.

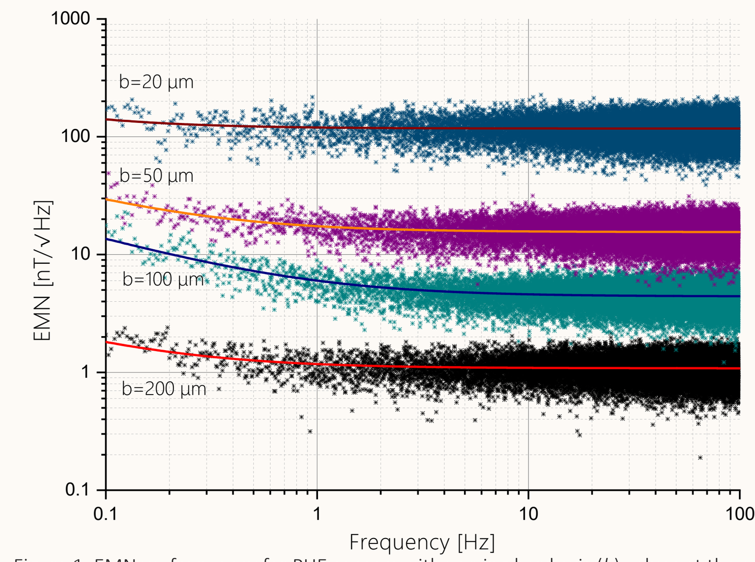


Figure 1. EMN vs. frequency for PHE sensors with varying hard axis (*b*) values at the same current density.

Figure 1 shows the EMN from 0.1 to 100 Hz for sensors with varying hard axis values. The EMN is fitted using:

$$\mathrm{EMN}(f) = \sqrt{B^2 + \frac{A^2}{f}}$$

where *A* and *B* are fitting parameters. At 10 Hz, the EMNs are approximately 1.1, 4.4, 16, and 117 nT/√Hz for hard axis values of 200, 100, 50, and 20 microns, respectively.

Notably, doubling the current density results in EMNs of 56 nT/√Hz and 7.7 nT/√Hz at 10 Hz for the 20-micron and 50-micron sensors, respectively.

Figure 2 shows the extended field range of the sensors in response to a magnetic field along the hard axis. The resistivity was measured during both ascending and descending fields and compared to the theoretical fit from the Stoner–Wohlfarth model:

$$R_{PHE} = \frac{\Delta R_{PHE}}{H_{eff}} \cdot H\sqrt{1 - \left(\frac{H}{H_{eff}}\right)^2}$$

The inset shows scaled data with normalized values.

It is evident that although all sensors exhibit non-linear behavior, this behavior can be precisely modeled, which means that they effectively behave as single magnetic domains.

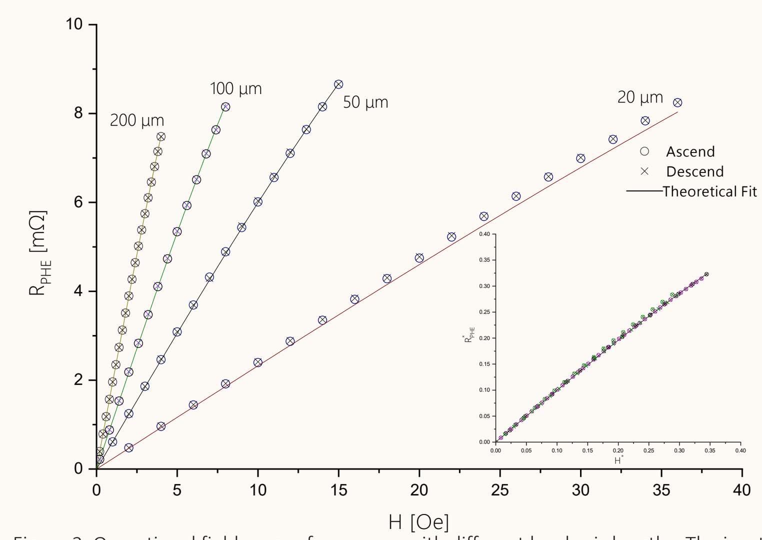


Figure 2. Operational field ranges for sensors with different hard axis lengths. The inset presents scaled data with normalized values.

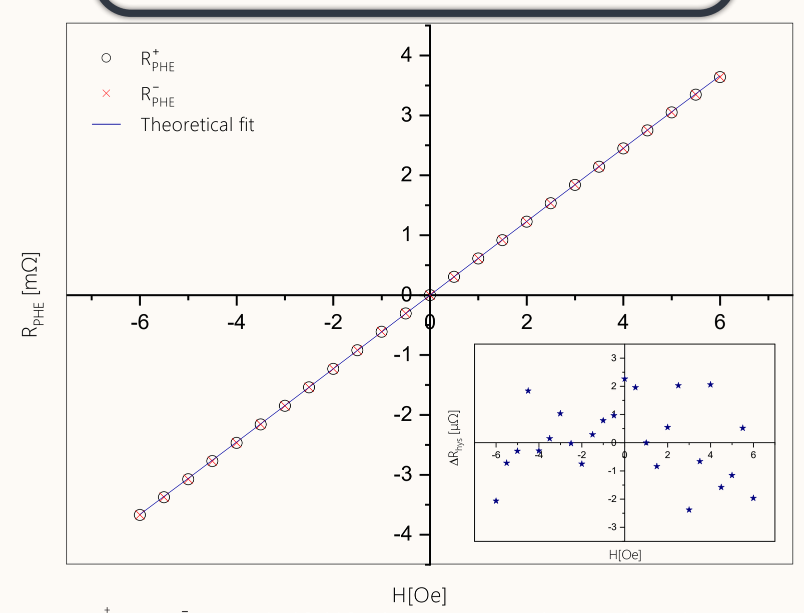


Figure 3. $R^+_{PHE}$ and $R^-_{PHE}$ vs. applied field for the 50μm sensor. The inset shows the resistivity difference between decreasing from +14 Oe and increasing from −14 Oe.

To evaluate hysteresis for a sensor with *b*=50μm, $R_{PHE}$ was measured in a −6 Oe to +6 Oe field range (linearity deviation < 1%) with 0.5 Oe steps.

Measurements were taken by reducing the field from +14 Oe ($R^+_{PHE}$) and increasing it from −14 Oe ($R^-_{PHE}$).

Figure 3 shows $R^+_{PHE}$ and $R^-_{PHE}$ , with the inset displaying $\Delta R_{hys}$= $R^+_{PHE} - R^-_{PHE}$.

Significantly, $\Delta R_{hys}$ changes sign, indicating that the differences are largely unrelated to magnetic hysteresis. Nevertheless, $\Delta R_{hys}$ can still be considered an upper bound for any potential magnetic hysteresis.

## 5 Conclusions

We demonstrated that extending the field range of EPHE sensors by increasing the ratio of thickness to the short axis significantly enhances their performance. Sensors with anisotropy fields of 12–120 Oe achieved EMNs of 800 pT/√Hz to 56 nT/√Hz, exhibiting stable single-domain behavior with negligible hysteresis.

These advancements make EPHE sensors promising for precise magnetic sensing in applications requiring extended field ranges, such as automotive and industrial systems.

Scan For More